INT. J. NUM. METH. HEAT FLUID FLOW, VOL. 3, 223–231 (1993)

NUMERICAL SIMULATION OF TWO-DIMENSIONAL COMPRESSIBLE FLOWS

J. F. MILTHORPE

Department of Mechanical Engineering, University College, University of New South Wales, Australian Defence Force Academy, Campbell, ACT 2600, Australia

ABSTRACT

A simple convection algorithm for simulation of time-dependent supersonic and hypersonic flows of a perfect but viscous gas is described. The algorithm is based on conservation and convection of mass, momentum and energy in a grid of rectangular cells. Examples are given for starting flow in a shock-tube and oblique shocks generated by a wedge, at Mach numbers up to 30.4. Good comparisons are achieved with well-known perfect gas flows.

KEY WORDS Compressible flows Convection algororithm

INTRODUCTION

Prediction of supersonic and hypersonic flows continues to be a significant problem, despite a great deal of work over many years. Some recent contributions have been made by, for example, Boris and Book[1], Löhner *et al.*[2], Chakravarthy *et al.*[3], Yee *et al.*[4] and Schmidt and Jameson[5]. Typical computation methods for the supersonic flow problem assume that the variables of the problem are continuous functions of space and time. Shocks are clear violations of the assumption of continuity. The most superficial acquaintance with Fourier analysis indicates the way in which a set of continuous functions will represent a discontinuity: by a series of wiggles around the discontinuity which decrease in amplitude with distance from the shock. The typical shock prediction demonstrates this behaviour perfectly. The more advanced algorithms include correction to suppress this behaviour. The traditional method for the prediction of supersonic flows is the method of characteristics. Based on the hyperbolic nature of the governing equations, this method allows reduction of the number of dimensions of the partial differential equation problem by one. Two-dimensional problems convert into the solution of ordinary differential equations along characteristic lines. The disadvantage of this method is the complexity of the process of evaluating the location of solution points from the intersection of the characteristic lines. A variant of the method of characteristics employs a fixed grid and assumes that the characteristics are piecewise straight. As a consequence the shocks are inaccurately located.

The error made by the classical type of algorithm is the assumption of continuity in discontinuous functions. The scheme advanced in this paper makes the opposite error: the solution functions are assumed to be discontinuous but the discontinuities are located in the wrong places. The algorithm used employs a primitive treatment of conserved flow quantities. This technique gives good results for supersonic flows described here, and promises relatively simple extension to reacting flows. The description of the algorithm will be preceded by a short description of a typical supersonic flow problem suitable for solution by this method, to convey the scope of the algorithm.

0961–5539/93/030223–09\$2.00

Received January 1993

TYPICAL SUPERSONIC FLOW PROBLEMS

The flow problems described in this paper are typical of those in the literature. A sample geometry, which exhibits most of the types of boundary condition in a fairly general form, is given in *Figure 1*, for flow over a wedge of half-angle 18.4°. The fluid enters the computational domain at the upstream surface A with given values of velocity, density, pressure, temperature and so on.

A feature which often appears is a symmetry surface or slip plane (B in *Figure 1*). There is no flow across this surface, no shear stress and no diffusion of energy or material. The flow values in any cell are, of course, only a representative average of the point values so non-zero velocities into the computational domain do not violate the condition of zero flow through the boundary. The velocity in the surface layer is required to be zero or into the domain, and no convection of mass is allowed across the boundary.

FREE DOWNSTREAM BOUNDARY CONDITIONS

The free downstream boundary condition, D in *Figure 1*, is by far the most difficult to implement successfully. The downstream condition which has proved successful with the algorithm described, in the test cases given, attempts to estimate the flow conditions outside the boundary from those just inside the boundary by projecting the contours of the flow variables across the boundary. This condition works well with the algorithm described here for both subsonic and supersonic outflow, as well as on the free stream boundary where the calculated outflow is approximately zero. This type of boundary condition would probably be unsuccessful in subsonic outflows with gradients in the flow, as would occur in a subsonic nozzle flow.

CONSERVATION ALGORITHM

The algorithm used to calculate the flow values is described fully in Milthorpe[6], together with a description of the computational resources required. A brief description is given here to indicate the basis of the method. The algorithm is based on conservation of mass, momentum and energy as the simulation proceeds over discrete timesteps. The flow domain is divided into rectangular cells. Each cell contains, at any given time, a certain block of material which possesses a certain

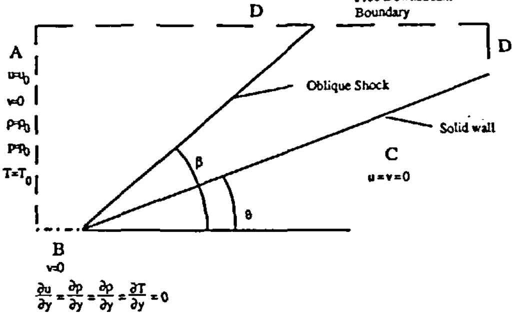

Figure 1 Example problem geometry, for supersonic flow over wedge with half-angle 18.4 degrees. The upstream flow conditions are fully specified and the downstream boundary condition is a projection of the solution across the boundary

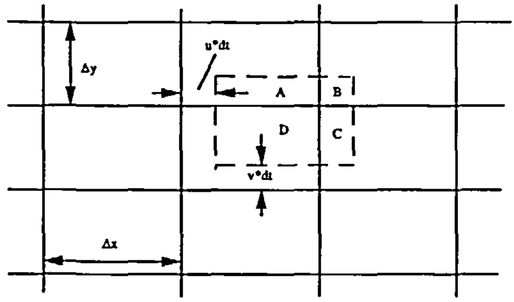

Figure 2 Convection of material block with velocity u, v during one timestep dt. See text for description of convection algorithm

momentum and energy. In the course of the next timestep this block, with its associated mass, momentum and energy, is convected a small distance. It may also gain or lose mass, momentum or energy by diffusion and the action of pressure gradients. The algorithm evaluates the changes in these quantities for the material block. The process is illustrated in *Figure 2* for convection with positive u and v velocities. The letters A, B, C, D represent the proportion of the material block located in a particular cell at the end of a timestep. These proportions of the quantities in the material block are allocated to their respective cells. When the process has been performed for all cells the new distribution of mass, momentum and energy is available. From this distribution updated values of density, velocity, pressure and temperature can be derived.

The algorithm used is based on an elementary treatment of conservation of flow properties. It is shown below to give accurate predictions of elementary compressible flows, although there are several algorithms available which give better results for perfect gas flows. The algorithm used here has the advantage that its simple treatment of conserved flow properties promises to make extension to multi-species flows and reacting flows a relatively simple process.

STABILITY LIMITS

Two limits are imposed on the size of the time-steps by stability considerations. The first is that the Courant number is less than one. The second limit is that due to over-prediction of diffusion, as described by Roache[7], which restricts the time-step Δt to:

$$\Delta t < \frac{\rho \Delta x^2}{2k} \tag{1}$$

where Δx is the step size, ρ the density and k the diffusion coefficient for any quantity.

TRANSIENT NORMAL SHOCK

The algorithm has been tested with a number of flows involving unsteady normal shocks at a range of Mach numbers. These flows represent a one-dimensional jet blowing into still gas: a typical established flow geometry is shown in *Figure 3*. The flow conditions were deliberately selected to give a mis-match between upstream and downstream values. As the density ratio

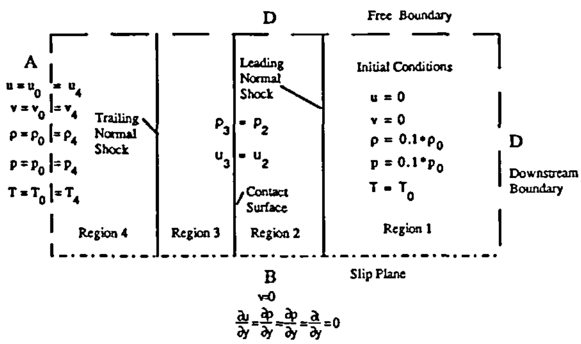

Figure 3 Example flow geometry, for supersonic flow with mis-matched upstream and downstream conditions. The upstream and downstream flow conditions are fully specified and the free stream and downstream boundary conditions are projections of the solution inside the flow field

across the shock system exceeds the limiting value, equal to 6 for air, the compression takes place in two stages. There is no limit on the density rise across the contact surface, as no gas flow occurs. The intermediate pressure, p_2 referring to the regions 1, 2, 3, 4 shown in *Figure 3*, is given by[8]:

$$\frac{p_4}{p_1} = \frac{p_2}{p_1}\left(1 - \frac{(\gamma_4 - 1)(a_1/a_4)(p_2/p_1 - 1)}{\sqrt{2\gamma_1}\sqrt{2\gamma_1 + (\gamma_1 - 1)(p_2/p_1 - 1)}}\right)^{-2\gamma/(\gamma-1)} \tag{2}$$

The other intermediate values follow from the pressure by the standard perfect gas equations[9]. It can be seen from *Figure 3* that, although the flow is one-dimensional, the algorithm is applied to a two-dimensional domain, with a symmetry plane on the lower surface and a free stream boundary on the upper surface, where the flow is projected to infinity. These conditions were selected to provide a thorough test for the algorithm. Results obtained for two widely separated Mach numbers are shown in *Figures 4* and *5*. In each Figure the perfect gas solution at the simulated time is superimposed on the calculated result. The grid used in the computations was

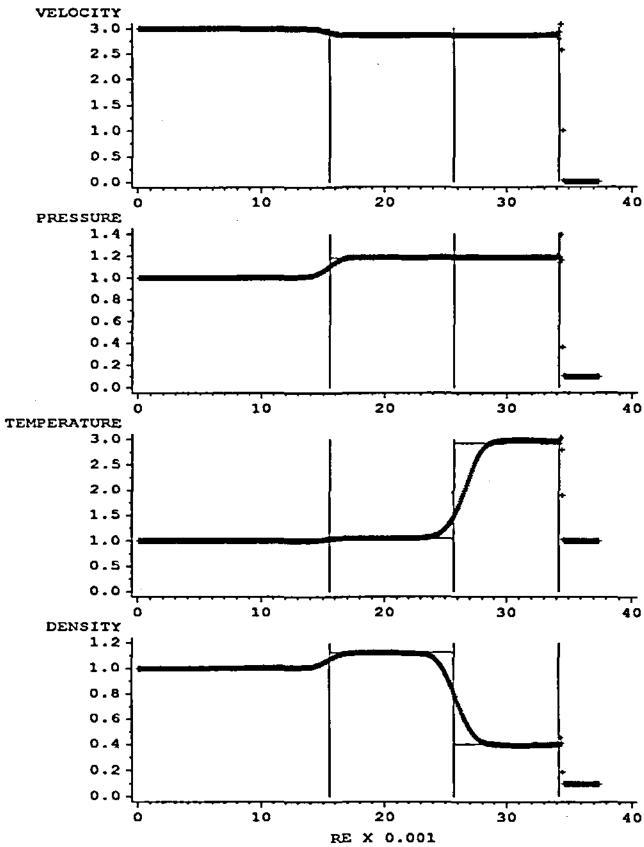

Figure 4 Mis-matched normal shocks moving into quiescent gas, with inlet Mach number $M_0 = 2.54$, at time $t_{nd} = 10649$. Pressure and density ratios are 10. The resultant incident shock Mach number is 3.208. The thin vertical lines indicate the position of the inviscid normal shocks and contact surface, and the thin horizontal lines the value of the inviscid solution between the shocks, at the same time

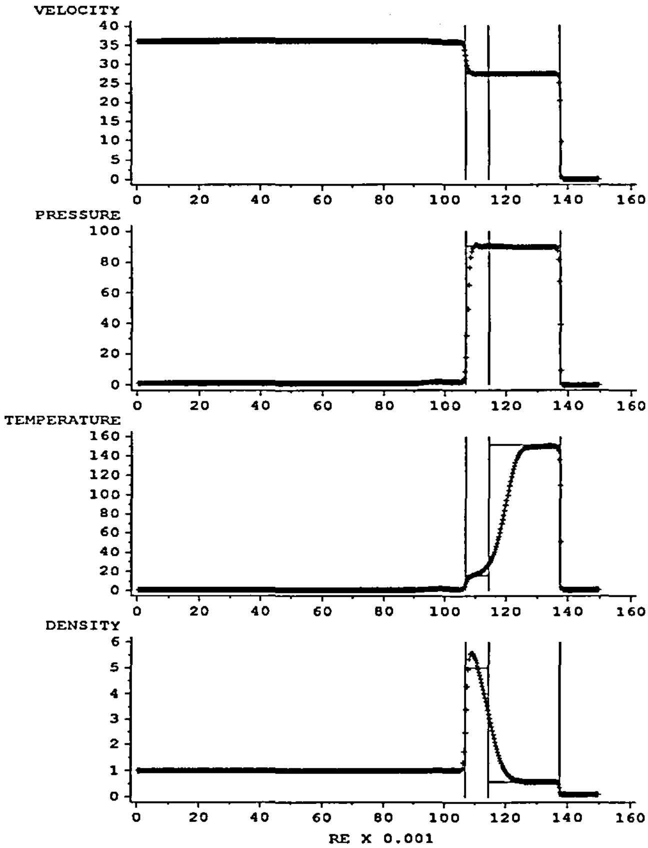

Figure 5 Mis-matched normal shocks moving into quiescent gas, with inlet Mach number $M_0 = 30.4$, at time $t_{nd} = 4970$. Pressure and density ratios are 10. The resultant shock Mach number is 32.95. The thin vertical lines indicate the position of the inviscid normal shocks and contact surface, and the thin horizontal lines the value of the inviscid solution between the shocks, at the same time

498 cells long by 28 cells wide, and the cells were squares of side 0.5. The abscissa in the Figures has a scale of Reynolds number:

$$Re = \frac{\rho_0 u_0 x}{\mu} \tag{3}$$

where ρ_0 is the inlet density, u_0 the inlet velocity, μ the dynamic viscosity of the gas and x the distance from the inlet boundary.

The non-dimensional time t_{nd} shown is given by:

$$t_{nd} = t \frac{\rho_0 u_0 a_0}{\mu} \tag{4}$$

where t is the time, and a_0 the inlet speed of sound. The wide variation in the Reynolds number scales and the non-dimensional times is due to the range of viscosities employed in the different tests.

The leading shock is sharply defined in all cases, while the contact surface and trailing shock are smeared out to some extent. In simulations begun with a sharply defined contact surface and trailing shock, the smeared result develops rapidly. The smearing is a product of the algorithm, but it remains to be checked whether the effect is caused by the simulated viscosity or by numerical diffusion.

The results shown demonstrate that, apart from the smearing of the contact surface and trailing shock, the algorithm accurately models the perfect gas theory at Mach numbers up to at least 30.4. The algorithm has not been tested at higher Mach numbers.

EXAMPLE PROBLEM

The problem shown in *Figure 1* has been used as an example to test the effectiveness of the algorithm. The particular reference values used were:

$$u_0 = 3.0 \tag{5}$$

$$\rho_0 = p_0 = T_0 = 1.0 \tag{6}$$

and the gas was taken as a perfect, but viscous, gas with:

$$\gamma = 1.4 \tag{7}$$

The viscosity, which varies with temperature according to Sutherland's law, was set at the lowest value which would give stable solutions.

The steady state upstream Mach number M_0 of the flow is thus 2.54. The deflection angle θ in inviscid flow would be 18.4°. The angle of the oblique shock β, and the downstream pressure p_1, density ρ_1, temperature T_1 and Mach number M_1 are standard results[9].

Contours of pressure and temperature for Mach = 2.54 are shown in *Figures 6–9*. Results are given while the flow is developing and when a steady state has been reached. The results are very similar to the inviscid predictions except for the presence of the boundary layer. There is a small curved detached shock at the apex of the wedge. The presence of the boundary layer results in a deflection angle slightly larger than that due to the wedge alone, and hence the flow variable after the shock do not have the inviscid values. A test of the accuracy of the algorithm is to examine the change in flow variables normal to the oblique shock, and compare these with the corresponding inviscid solution. This has been done in *Figure 10*. The shock angle was

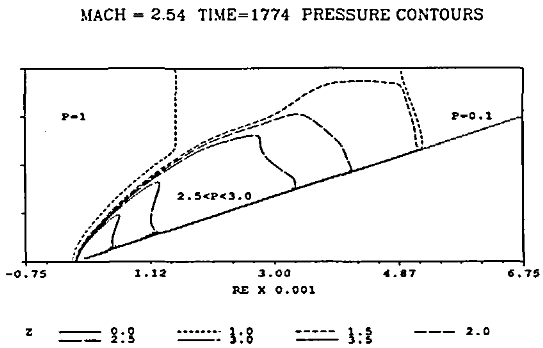

Figure 6 Mach number contours in transient flow over a wedge of half-angle 18.4° with incident Mach number 2.54. Mis-matched normal shocks are moving into quiescent gas at time $t_{nd} = 1774$. Pressure and density ratios are 10

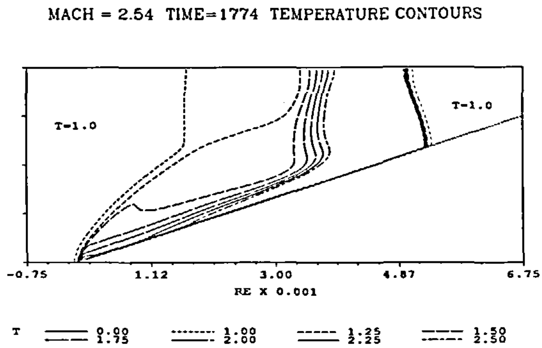

Figure 7 Temperature contours in transient flow over a wedge of half-angle 18.4° with incident Mach number 2.54. Mis-matched normal shocks are moving into quiescent gas at time $t_{nd} = 1774$. Pressure and density ratios are 10

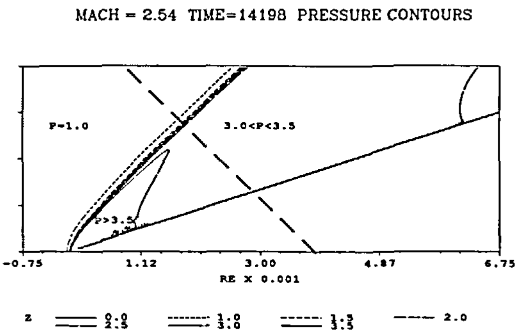

Figure 8 Pressure contours in transient flow over a wedge of half-angle 18.4° with incident Mach number 2.54. Time $t_{nd} = 14198$. ---, Reference line for flow values in *Figure 10*

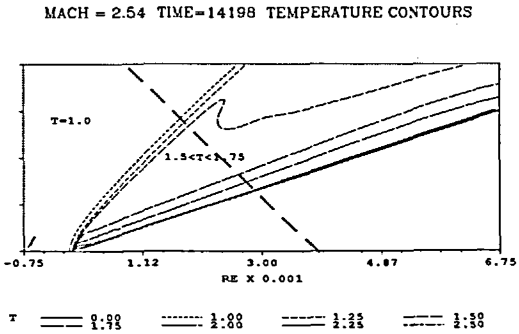

Figure 9 Temperature contours in transient flow over a wedge of half-angle 18.4° with incident Mach number 2.54. Time $t_{nd} = 14198$. ---, Reference line for flow values in *Figure 10*

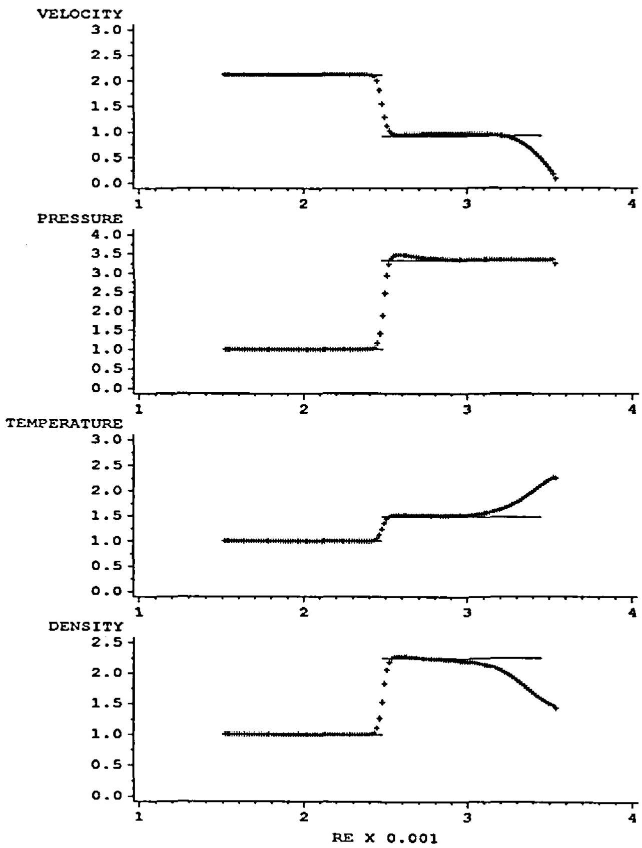

Figure 10 Flow values in a line perpendicular to the oblique shock, Mach number 2.54, shown in *Figures 8–9*. The thin horizontal lines indicate the value of the inviscid variables across an oblique shock of the same angle

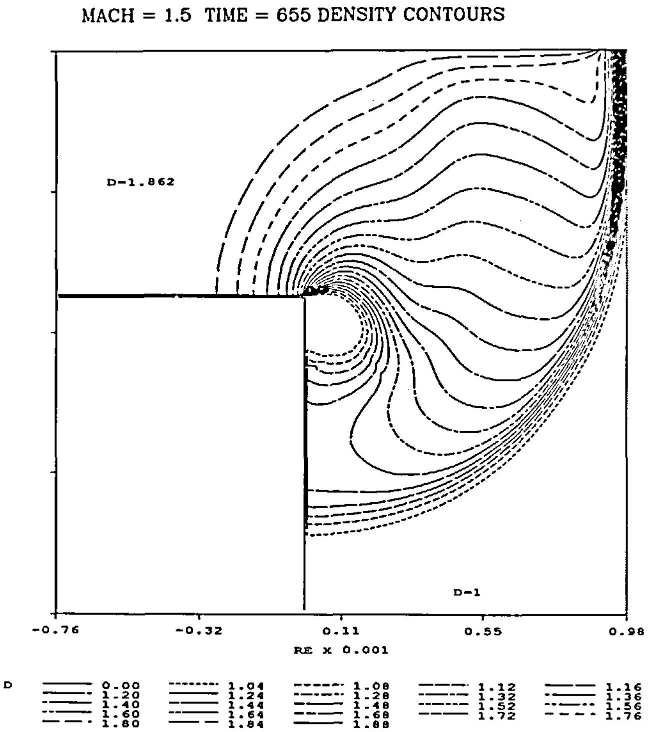

Figure 11 Density contours in expansion over a right angle corner with incident shock Mach number 1.77. Time $t_{nd} = 655$

measured as 43°. It can be seen that the computation is very close to the inviscid values for this deflection angle near the shock.

EXPANSION OVER REARWARD FACING STEP

The flow over a rearward facing step is a popular problem in both compressible and incompressible fluid dynamics. The particular configuration shown here was proposed by Takayama[10] for Euler codes and shows a shock wave diffracted over the step. Relative to the initial conditions, the flow conditions at the upstream inlet are pressure ratio 2.4583, density ratio 1.86207. The velocity at the upstream inlet is selected to give an incident shock Mach number of 1.77 and the gas modelled is a perfect gas with $\gamma = 1.4$. The Reynolds number based on the length upstream of the step is 765. As a slip boundary condition is applied at the walls no boundary layer is formed and the Reynolds number scale is only significant for the thickness of the shock. The density contours calculated are given in *Figure 11*. The grid used was 232 by 232 cells.

CONCLUSION

The algorithm described gives satisfactory simulations of viscous, perfect gas flows at Mach numbers ranging from low supersonic to hypersonic values. The algorithm has the potential to be developed to incorporate real gas effects created by dissociation and recombination of molecules in high enthalpy flows, and further work will proceed in this direction.

REFERENCES

1 Boris, J. P. and Book, D. L. Flux-corrected transport, I. SHASTA, a fluid transport algorithm that works, *J. Comput. Phys.* **11**, 38–69 (1973)
2 Löhner, R., Morgan, K., Peraire, J. and Vahdati, M. Finite element flux-corrected transport (FEM–FCT) for the Euler and Navier–Stokes equations, *Int. J. Num. Meth. Fluids* **7**, 1093–1110 (1987)
3 Chakravarthy, S. and Osher, S. A new class of high accuracy TVD schemes for hyperbolic conservation laws, *AIAA Pap. 85-0363* (1985)
4 Yee, H. C., Warming, R. F. and Harten, A. Implicit total-variation diminishing (TVD) schemes for steady state calculations, *J. Comput. Phys.* **57**, 327–360 (1985)
5 Schmidt, W. and Jameson, A. Euler solvers as an analysis tool for aircraft aerodynamics, in *Advances in Computational Transonics* (Ed. W. G. Habashi), pp. 371–404, Pineridge Press, Swansea (1985)
6 Milthorpe, J. F. Simulation of supersonic and hypersonic flows, *Int. J. Num. Meth. Fluids* **14**, 267–288 (1992)
7 Roache, P. J. *Computational Fluid Dynamics*, Hermosa Publishers, Albuquerque, pp. 279–282 (1976)
8 Mudford, N. R. Supersonic flows with fully specified properties entering a stagnant region with fully specified properties, personal communication (1989)
9 Liepmann, H. W. and Roshko, A. *Elements of Gasdynamics*, John Wiley, New York (1957)
10 Takayama, K. personal communication (1991)